05,12

Natural Ferromagnetic Resonance in y-Fe₂O₃ and CoFe₂O₄ Nanopowders

© S.V. Stolyar^{1,2,3}, I.G. Vazhenina^{1,3}, A.O. Shokhrina^{1,2}, E.D. Nikolaeva¹, N.M. Boev³, O.A. Li^{1,2}, R.S. Iskhakov³, A.M. Vorotynov³, D.A. Velikanov³, M.N. Volochaev³, A.D. Vasiliev³

¹ Krasnoyarsk Scientific Center of the Siberian Branch of the Russian Academy of Sciences, Krasnoyarsk, Russia

Krasnoyarsk, Russia

Krasnoyarsk, Russia

³ Kirensky Institute of Physics, Siberian Branch of the Russian Academy of Sciences — separate division Federal Research Center — Krasnoyarsk Scientific Center, Siberian Branch of the Russian Academy of Sciences,

E-mail: stol@iph.krasn.ru Received March 6, 2025 Revised March 6, 2025 Accepted May 5, 2025

 γ -Fe₂O₃ and CoFe₂O₄ nanopowders were prepared by the chemical precipitation method. Magnetization curves, ferromagnetic resonance curves, and dependences of the temperature of the powders on time were measured during the absorption of microwave field energy at a frequency of 8.9 GHz at different values of the magnetic field strength. It was found that the greatest temperature increment of cobalt ferrite powders is achieved in the absence of an applied constant magnetic field — at natural ferromagnetic resonance. The frequencies of natural ferromagnetic resonance of the prepared powders were determined. Heating of magnetic nanoparticles in the field of their magnetic anisotropy (natural ferromagnetic resonance) can find application in biomedicine.

Keywords: magnetic nanoparticles, ferromagnetic resonance, natural ferromagnetic resonance.

DOI: 10.61011/PSS.2025.06.61707.17HH-25

1. Introduction

Due to their unique properties, magnetic nanoparticles are used for many applications, including biomedicine. Promising biomedical applications of magnetic particles include magnetic separation, magnetic hyperthermia, targeted delivery of medicinal agents, magnetic resonance imaging [1,2]. Possibility to convert the absorbed energy of an alternating magnetic field into heat makes it possible to use nanomaterials on the basis of magnetic nanoparticles as thermal agents for controlled local heating in tumor therapy [3,4].

In [5,6], authors propose a new heating method for biomedical applications on the basis of the ferromagnetic resonance phenomenon.

Ferromagnetic resonance (FMR) is intensive absorption of the microwave field energy that takes place when the applied dynamic field frequency is equal to the magnetization vector precession frequency of powder nanoparticles around the direction of the effective magnetic field \overrightarrow{H}_{eff} induced in the sample. Macroscopic description of FMR is provided by the Landau–Lifshitz–Gilbert equation [7]:

$$\dot{\vec{M}} = -\gamma \vec{M} \times \vec{H}_{eff} - \gamma \frac{\alpha}{M} \vec{M} \times (\vec{M} \times \vec{H}_{eff}), \qquad (1)$$

where \overrightarrow{M} is the instantaneous value of the magnetization vector in the effective (internal) magnetic field, γ is the gyromagnetic ratio, α is the damping parameter. In

the simplest case, the effective field is H_{eff} , that is expressed through magnetic energy density according to $\overrightarrow{H}_{eff} = -\partial U/\partial \overrightarrow{M}$, is composed of the external field \overrightarrow{H} , internal anisotropy field \overrightarrow{H}_K of the ferromagnetic material and demagnetizing field of the sample.

Resonance energy absorption occurs in the situation when the ferromagnetic magnetization \overrightarrow{M} is exposed, besides the permanent field \overrightarrow{H}_{eff} , to the perpendicular microwave field \overrightarrow{h} with frequency ω and amplitude h_0 , and it is this that induces heating of the test sample [8,9].

A so-called natural resonance is one of the varieties of FMR. It occurs in the absence of an external field and is typical of powders whose particles have a strong internal magnetic anisotropy field. Resonance frequency in this case is $\omega_0 = \gamma H_K$, and the damping time of magnetization precession \overrightarrow{M} is determined by the following expression

$$\tau_0 = (\alpha \omega_0)^{-1} = M/2\alpha \gamma K, \qquad (2)$$

where K is the magnetic anisotropy energy density, $K = MH_K/2$.

From a practical point of view, local heating using the natural ferromagnetic resonance is most preferable for biomedicine applications because only alternative electromagnetic microwave field is required for implementing the natural ferromagnetic resonance (i.e. permanent magnetic fields are not required). The microwave field itself has

² Siberian Federal University,

a heating effect on biological tissues, while the depth of wave penetration in tissues depends on the frequency f of the employed radiation. For $f=10\,\mathrm{GHz}$, the depth of penetration in marrow is 3.4 mm, in brain is 1.6 mm, in fat tissue is 11 mm, in skin is 1.9 mm [10]. Small penetration depth of microwave radiation is a major advantage because the effect turns out to be local and the "Brezovich limit" problem is eliminated [11]. To supply electromagnetic energy deep into the tissue, emitters in the form of a "microwave syringe" may be used [12].

In single-domain ferromagnetic particles, thermofluctuation (superparamagnetic) effect has a considerable influence on the magnetic moment motion $\overrightarrow{m} = \overrightarrow{M}V$, where V is the particle volume. It becomes perceptible in a size region where the magnetic anisotropy energy KV is commensurate with the heat energy k_BT . In this case, the magnetic moment is able to overcome the potential barrier KV by means of fluctuation and, thus, is involved in the orientation diffusion process characterized by the relaxation time.

$$\tau_D = MV/(2\alpha\gamma k_{\rm B}T). \tag{3}$$

This is a limit to which the Neel (exponential) time tends to as the potential barrier height reduces to zero, see, for example [13]. In small particles, the imaginary part of dynamic susceptibility χ'' will be defined by the ratio of the values of τ_D and τ_0 , between which there is a simple relation [14]:

$$\tau_D = \sigma \tau_0, \quad \sigma = KV/k_BT.$$
 (4)

At $\tau_D > \tau_0$, $\sigma > 1$, the microwave field absorption line is of a resonance type. At $\tau_D < \tau_0$, $\sigma < 1$, the absorption line becomes a relaxation one. Since the absorbed power P is proportional to the imaginary part of magnetic susceptibility $P \sim \chi''$, then experimental determination of the dynamic susceptibility behavior is an essential issue for solution of magnetic hyperthermia application problems.

This study uses $CoFe_2O_3$ and γ -Fe₂O₃ powders to demonstrate that the natural ferromagnetic resonance condition may be implemented in these objects and, thus, particle heating may be provided.

2. Experiment procedure

 $\gamma\text{-Fe}_2O_3$ powders as well as CoFe_2O_4 powders were prepared by the chemical deposition method. The essence of the method is in deposition of divalent and trivalent iron in the ratio of 2 to 1 with addition of alkali. To prepare cobalt ferrite, 0.2 mole $\text{CoSO}_4 \times 7\text{H}_2\text{O}$, and 0.4 mole $\text{FeCl}_3 \times 6\text{H}_2\text{O}$ were dissolved in 100 ml dH₂O, NH₄OH was added dropwise up to pH = 11 and heated with continuous stirring to 80 °C during 30 min. Then the precipitate was washed. The synthesized CoFe_2O_4 powders at 700 °C were annealed during 5 h to increase the particle size. Annealing was performed in a muffle furnace (SNOL-16251/11-IZ.) in air. The furnace was turned off after annealing. The

powder was cooled together with the furnace. Natural sintering and recrystallization processes take place during the annealing process, consequently the particle size increases. The resulting material was triturated in a mortar. X-ray diffraction analysis was performed using the DX-2700BH, HAOYUAN, DRON-4 $\lambda = 0.154 \, \text{nm}$ instruments. Sizes of the prepared powders were examined using the Hitachi HT7700 transmission electron microscope (accelerating voltage 100 kV). Static magnetic properties of the powders were measured using the LakeShore VSM 8604 vibrating magnetometer at room temperature. FMR curves at different temperatures were measured using the Bruker EPR spectrometer ($f = 9.4 \,\mathrm{GHz}$). Particles were heated in microwave field pumping conditions at room temperature using the SE/X-2544 (Radiopan) ($f = 8.9 \,\text{GHz}$) EPR spectrometer. Sample temperature was measured using a T type thermocouple with copper and constantan electrodes. Powder weight was about 10 mg. The thermocouple didn't detect any temperature variations in the empty cavity with microwave filed pumping and bias field scanning from 0 to 5 kOe. The imaginary part μ'' of the permeability of the prepared powder was measured using a broadband ferromagnetic resonance spectrometer at 300 K in a frequency band from 100 MHz to 10 GHz [15].

3. Results and discussion

Figure 1 shows X-ray images and reflection identification of the freshly prepared CoFe₂O₄ powder, annealed CoFe₂O₄ powder and γ-Fe₂O₃ powder. Evaluation of the coherent scattering region (CSR) using the Scherrer equation gave the following results: for the freshly prepared CoFe₂O₄ powder — 3 nm, heat-treated powder — 17 nm, for the γ -Fe₂O₃ powder — 8 nm. TEM images were used to evaluate particle size distribution and the mean particle Size distribution of freshly prepared CoFe₂O₃ powders is characterized by two modes at $d_1 \approx 4 \,\mathrm{nm}$ and $d_2 \approx 11 \,\mathrm{nm}$, annealing of this powder leads to an increase in sizes to $d_3 \approx 23$ nm. Mean particle size of the γ -Fe₂O₃ powder is $d_4 \approx 8$ nm. It is virtually impossible to distinguish maghemite, y-Fe₂O₃, from magnetite, Fe₃O₄, using diffraction methods due to the closeness of their lattice parameters. It is shown in [16] that iron oxide particles larger than 60 nm have a crystal structure and exhibit physical properties of bulk magnetite. Smaller iron oxide nanoparticles represent a nonstoichiometric magnetitemaghemite compound with the crystallochemical formula $\operatorname{Fe}^{3+}[\operatorname{Fe}_{1-3n}^{2+}\operatorname{Fe}_{1+2n}^{3+}\phi_n]O_4$, where ϕ is the designation of vacancies, n is the formula coefficient. When the particle size is smaller than 10 nm, the maghemite phase prevails. In our case, the mean particle size doesn't exceed 10 nm, therefore, the γ -Fe₂O₃ phase shall prevail. These powders were also used to measure Mössbauer spectra according to which Fe ions are exclusively in the F³⁺state indicating the presence of the γ -Fe₂O₃ phase.

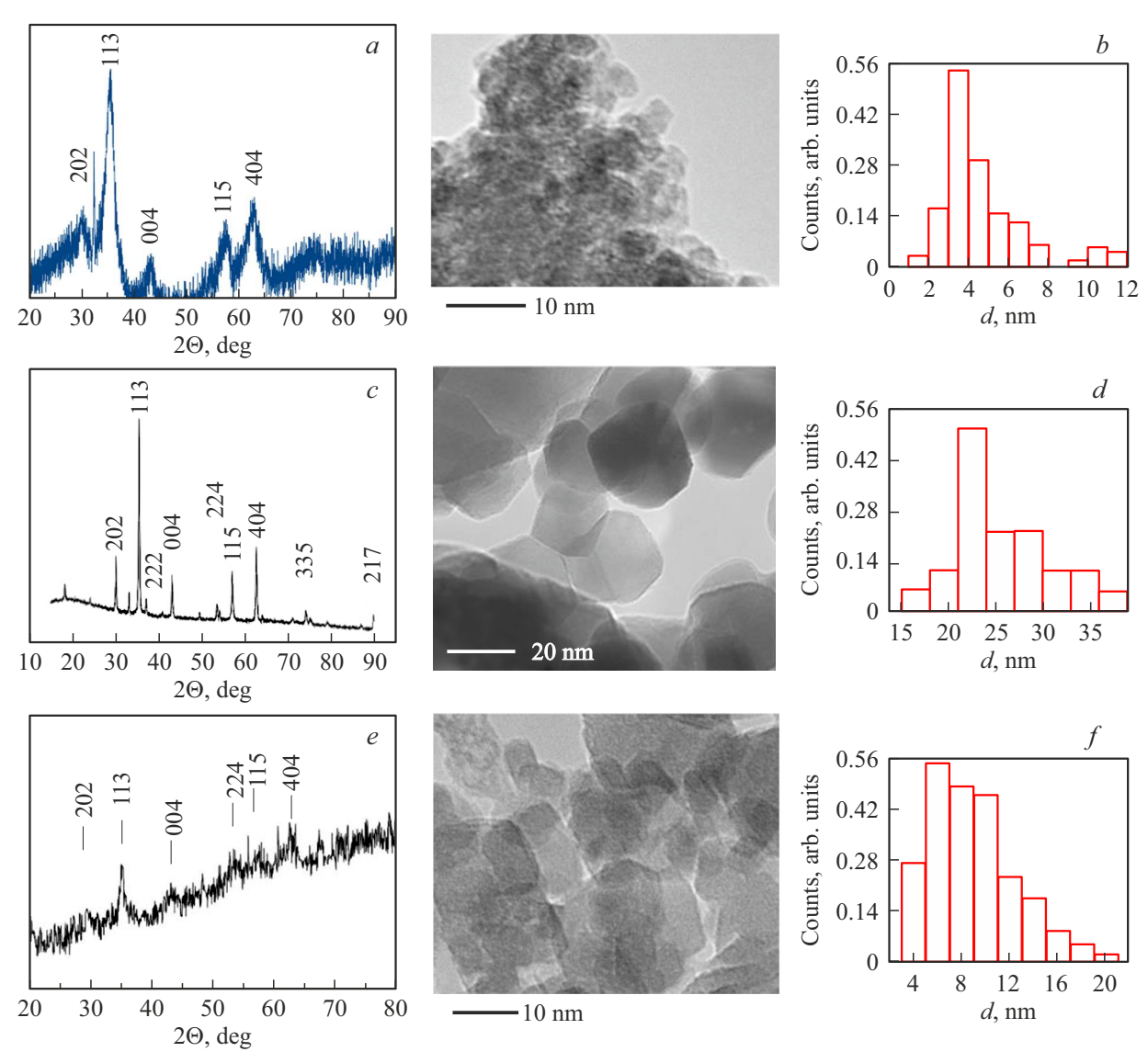


Figure 1. Findings of the structural determination of powders. X-ray and TEM images of the freshly prepared CoFe₂O₄ powder (a and b), heat-treated CoFe₂O₄ powder (c and d), γ -Fe₂O₃ powder (e and g) and their size distribution (TEM), respectively.

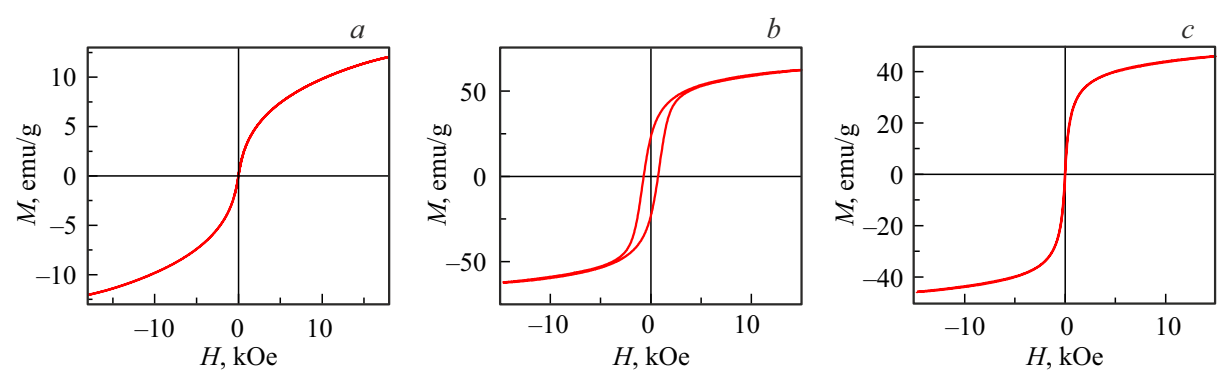


Figure 2. Remagnetization curves M(H) of the freshly prepared CoFe₂O₄powder (a), heat-treated CoFe₂O₄ powder (b) and γ -Fe₂O₃ powder (c).

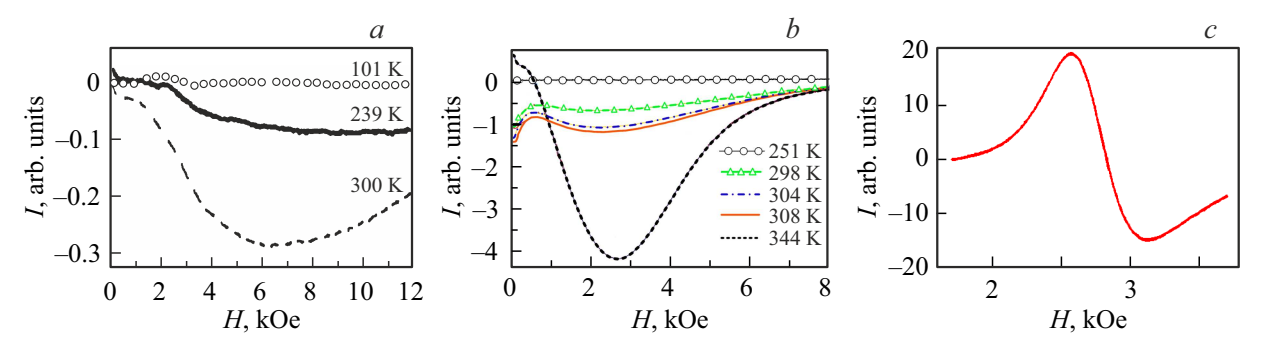


Figure 3. Differential FMR curves of the prepared powders at different temperatures recorded at 8.9 GHz of: (a) the freshly prepared $CoFe_2O_4$ powder, (b) heat-treated $CoFe_2O_4$ powder and (c) γ -Fe₂O₃ powder.

Sample	d, nm	ρ , g/cm ³	H _C , Oe		H_r , kOe $(f = 8.9 \text{GHz}, T = 300 \text{K})$	ΔH , kOe $(f = 8.9 \text{GHz}, T = 300 \text{K})$	ΔT_{max} , K $(f = 8.9 \text{GHz}, T = 300 \text{K})$
CoFe ₂ O ₄ Initial	4 11	5.2	5	12	≈ 0	12	11
CoFe ₂ O ₄ annealed	23	5.2	720	64	≈ 0	≈ 4	13
γ-Fe ₂ O ₃	8	4.8	14	47	2.8	0.56	11

Table 1. Sizes and magnetic parameters of powders

Remagnetization curves M(H) recorded at room temperature for the prepared powders are shown in Figure 2. M(H) of the freshly prepared CoFe₂O₄ powder (Figure 2, a) is typical for a superparamagnet and is a Langevin dependence with a small "ferromagnetic" additive. that there is no saturation in the employed magnetic field range (up to 18 kOe) for the freshly prepared CoFe₂O₄ powder. Static magnetic measurements (magnetization M, coercive force H_C) are shown in Table 1. Magnetization M was measured at $H = 18 \,\mathrm{kOe}$. Analysis of the M(H)data for the heat-treated CoFe₂O₄ powder suggests the formation of a magnetically hard material. Increase in the magnetization after heat treatment may be associated with a decrease in the specific surface of the powder after annealing. Magnetoactive atoms on the surface (near the surface) form a "dead magnetic layer". After annealing, the number of such atoms per unit volume decreases leading to an increase in the magnetization. Static magnetic properties of the studied γ -Fe₂O₃ powder comply with the properties of powder with similar sizes from [17].

Figure 3 shows differential FMR curves of the prepared powders at different temperatures recorded at 8.9 GHz. Measurements for cobalt ferrite both in the freshly prepared state (Figure 3, a) and heat-treated state (Figure 3, b) indicate that there is almost no microwave energy absorption of the powders in the FMR mode up to room temperatures. The resonance absorption curve of the freshly prepared powder at $T=300\,\mathrm{K}$ has the resonance field $H_r\approx 0\,\mathrm{Oe}$ and the line width ΔH more than $10\,\mathrm{kOe}$ (Figure 3, a). Heat treatment of cobalt ferrite powder leads to a threefold

decrease in ΔH . Magnetic parameters measured by the dynamic method are listed in Table 1. In our view, high values of the FMR line width for cobalt ferrite are defined by the concentration distribution inhomogeneity of cobalt and iron cations Mössbauer reported by the Mössbauer investigations [18]. Apparently, not only recrystallization processes, but also ordering processes take place after heat treatment. The absence of resonance absorption at low temperatures indicates that there is a temperaturedependent gap of the FMR frequency-field dependence of the cobalt ferrite powders. In the natural FMR conditions, the magnitude of gap is defined by the anisotropy field $H_K = \omega_0/\gamma \approx 3$ kOe. FMR curve parameters (shape, resonance field, line width, intensity) of the γ -Fe₂O₃ powder remained almost unchanged in the given temperature range. Figure 3, c shows a differential absorption curve of the γ-Fe₂O₃ powder measured at room temperature. FMR curve parameters (resonance field H_r and line width ΔH) for each test sample are listed in Table 1.

Figure 4 shows kinetic temperature increment curves of the prepared powders in various magnetic fields. Values of maximum heating $\Delta T_{\rm max}$ for each measured powder are listed in Table 1. Increase in ΔT of the ${\rm CoFe_2O_4}$ powder after annealing is caused by an increase in M because $\Delta T \sim M$ [8]. For ${\rm CoFe_2O_4}$ powders both in the freshly prepared state and after heat treatment, maximum heating is recorded with no external magnetic field. As the external field strength increases, ΔT decreases. This is associated with the fact that the natural ferromagnetic resonance frequencies for the freshly prepared and heat-treated cobalt

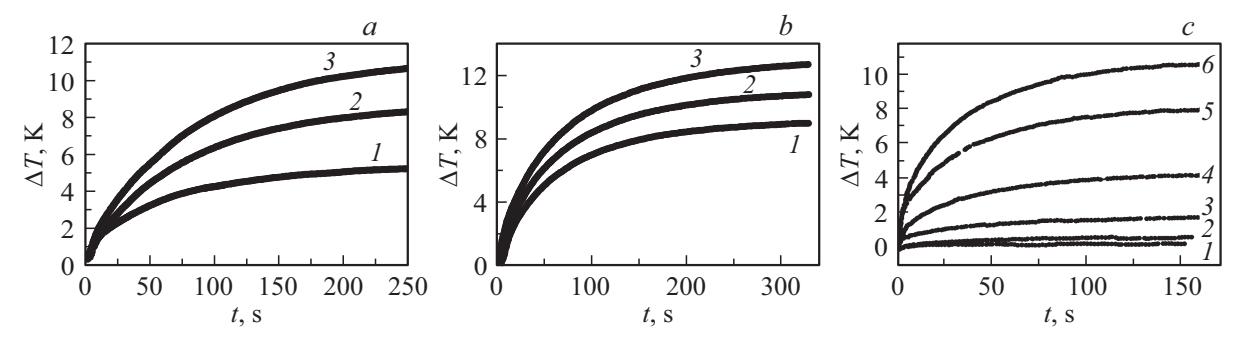


Figure 4. Kinetic temperature increment curves of the prepared powders in various magnetic fields. (a) $\Delta T(t)$ of the freshly prepared CoFe₂O₄ powder, where curve *I* was recorded at the external field $H=6\,\mathrm{kOe}$, $2-H=3\,\mathrm{kOe}$, $3-H=0\,\mathrm{kOe}$; (b) $\Delta T(t)$ of the heat-treated CoFe₂O₄ powder, where curve *I* was recorded at the external field $H=10\,\mathrm{kOe}$, $2-H=5\,\mathrm{kOe}$, $3-H=0\,\mathrm{kOe}$; (c) $\Delta T(t)$ of the γ -Fe₂O₃ powder, where curve *I* was recorded at the external field $H=0\,\mathrm{kOe}$, $2-H=1.5\,\mathrm{kOe}$, $3-H=2\,\mathrm{kOe}$, $4-H=3.7\,\mathrm{kOe}$, $5-H=3.4\,\mathrm{kOe}$, $6-H=2.8\,\mathrm{kOe}$.

ferrite powders are close to the frequency used for heating measurement. At $f = 8.9 \,\mathrm{GHz}$, the internal effective field $H_{eff} = 2\pi f/\gamma \approx 3$ kOe. During application of the external magnetic field H, we change the effective field $H_{eff} = 2\pi f/\gamma + H$, and, therefore, leave the resonance condition. In other words, in the resonance condition, the imaginary part of χ'' has its maximum value. The natural ferromagnetic resonance condition H = 0, therefore χ'' $(H = 0) > \chi''(H)$. Power P absorbed by the magnetic powder is determined as $P = \omega \frac{V}{2} \chi'' h^2$, V is the particle volume, h is the microwave field amplitude. And since $P \sim \Delta T$, then a decrease in the powder heating temperature with an increase in the external magnetic field is natural. Thus, the natural FMR excitation that occurs without an external magnetic field turns out to be the best condition for heating the CoFe₂O₄ powders. ΔT_{max} for the γ -Fe₂O₃ powder is $\approx 11 \,\mathrm{K}$ at $H_r \approx 2.8 \,\mathrm{kOe}$. With deviation from the resonance field in any direction, the heating value decreases.

Natural FMR frequency f_0 of the studied powders was determined by the measured frequency dependences of the imaginary component of the permeability $\mu'' \approx 4\pi\chi''$ that are shown in Figure 5. For the freshly prepared CoFe₂O₄ powder, curve $\mu''(f)$ has two features in the low-frequency and high-frequency regions (Figure 5, a). At $f_0 = 7.5\,\text{GHz}$, a resonance type of absorption is recorded. Using the gyromagnetic ratio $\gamma/2\pi = 2.9\,\text{GHz/kOe}$, the magnetic anisotropy field $H_K \approx 2.6\,\text{kOe}$ may be determined. Then $M = 50\,\text{G}$ determined from the static measurements (see Figure 2, a, Table 1) for the freshly prepared CoFe₂O₄ powder and $K = MH_K/2$ are used to determine the magnetic anisotropy constant $K \approx 6.5 \cdot 10^4\,\text{erg/cm}^3$. At low frequencies $f_0 \approx 0.8\,\text{GHz}$ (Figure 5, a), a relaxation type of absorption is observed.

Since the particle size distribution of the freshly prepared CoFe_2O_4 powder is bimodal — $d_1 \approx 4 \, \text{nm}$ and $d_2 \approx 11 \, \text{nm}$, it is reasonable to associate the shape of curve $\mu''(f)$ with the powder particle size distribution. For small particles, we get $\sigma_1 = KV_1/k_BT \approx 0.05 < 1$, which corresponds to the relaxation absorption of the microwave field energy;

for larger particles, $\sigma_2 = KV_2/k_BT \approx 1.3 > 1$ corresponds to the resonance absorption of the microwave field energy. Evaluation of σ used $K \approx 6.5 \cdot 10^4 \, \mathrm{erg/cm^3}$ determined above from the parameters of curve $\mu''(f)$ at $f_0 = 7.5 \, \mathrm{GHz}$.

Expressions for χ'' for $\sigma < 1$ (relaxation type) and for $\sigma > 1$ (resonance type) were derived in [14]. Specifically at $\sigma < 1$ (low-frequency region in Figure 5, a):

$$\chi_1^{\prime\prime} = rac{\chi_0 \omega au_D}{1 + (\omega au_D)^2},$$

where

$$\chi_0 = \frac{M_1^2 V_1}{3k_D T};\tag{5}$$

at $\sigma > 1$ (high-frequency region), the result is given by the classical Landau and Lifshitz equation [8]:

$$\chi_2'' = \frac{\alpha \omega [(1 + \alpha^2) \cdot \omega_0^2 + \omega^2]}{[(1 + \alpha^2)\omega_0^2 - \omega^2]^2 + 4(\alpha \omega_0 \omega)^2},$$

where

$$\omega_0 = \gamma H_K = \gamma \, \frac{2K_2}{M_2} = 2\pi f_0. \tag{6}$$

5, a shows the fitting curve $\mu'' = 4\pi$ $\times (n_1 \chi_1'' + n_2 \chi_2'')$, where n_1 and n_2 are the specific contents of particle sizes in the accepted bimodal approximation of the powder phase composition. $n_1 = 0.9$ is the content of 6 nm particles, $n_2 = 0.1$ is the content of 11 nm particles. Other constitutive parameters used in (5) and (6) for calculation of fitting curve μ'' for cobalt ferrite powders are shown in Table 2. These parameters were used to plot a fitting curve (dashed line in Figure 5, a) that agrees adequately with the experimental curve $\mu''(f)$. $M_1 = 240 \,\mathrm{G}$ and $M_2 = 62 \,\mathrm{G}$ of the above-mentioned phases of the freshly prepared $CoFe_2O_4$ powder exceed $M = 50 \, G$, evaluated from the magnetization curves M(H). This may be caused by several factors. First, the curves M(H) were recorded at room temperature and the fitting parameters M_1 and M_2 describe the powder at T=0. Second, the utilized magnetic fields (H < 18 kOe) didn't lead to saturation of

Sample	f_0 , GHz	α	$V \cdot 10^{-19}, \text{ cm}^3$	d, nm	M, G	K, erg/cm ³	$\sigma = KV/k_{\rm B}T$	MV, emu
Initial CoFe ₂ O ₄	0.8	0.04	1.1	6	240	$1 \cdot 10^4$	0.02	$2.4 \cdot 10^{-17}$
mittai Core ₂ O ₄	7.5	0.19	6.7	11	62	$8 \cdot 10^4$	1.3	$4.1 \cdot 10^{-17}$
Heat-treated CoFe ₂ O ₄	8	0.15	82	25	350	$5 \cdot 10^5$	98	$2.8 \cdot 10^{-15}$
γ-Fe ₂ O ₃	1.2	0.22	2.7	8	190	$1 \cdot 10^5$	0.6	$5.1 \cdot 10^{-17}$

Table 2. Natural ferromagnetic resonance frequencies f_0 . Fitting parameters of experimental curves $\mu''(f)$

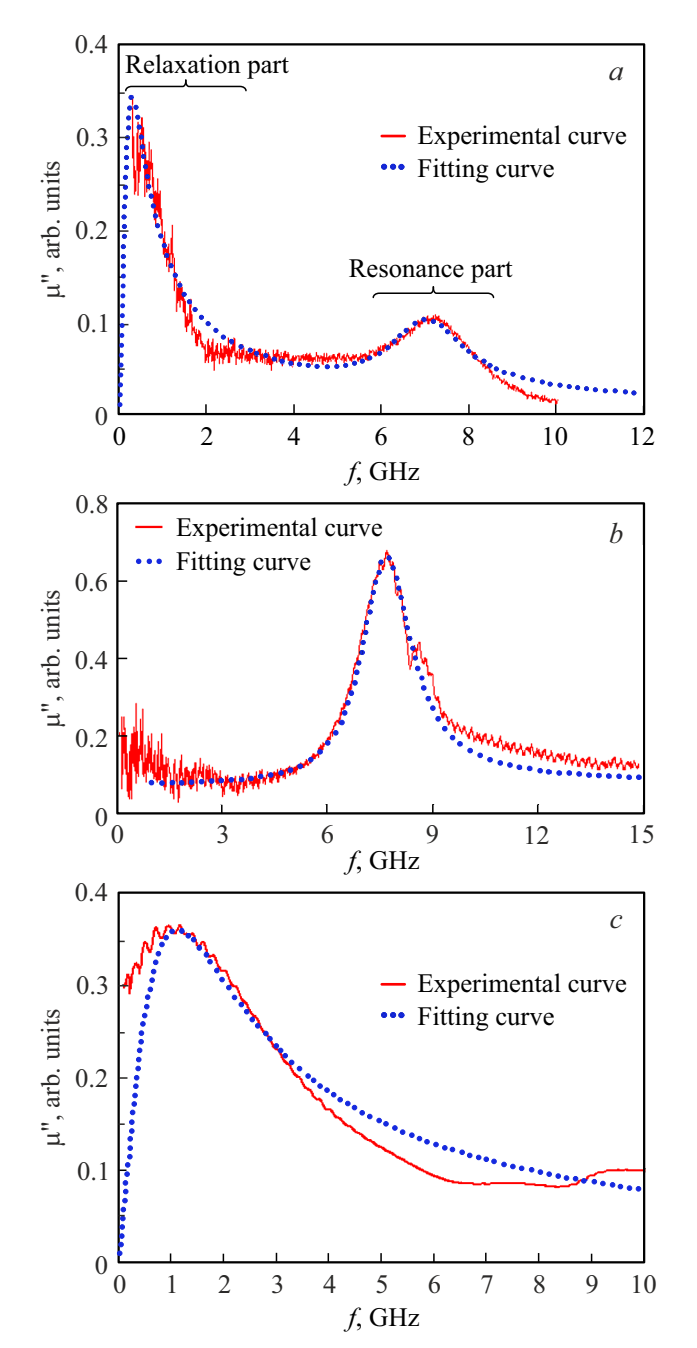


Figure 5. Frequency dependences of the imaginary component of the permeability of the freshly prepared $CoFe_2O_4$ powder (a), heat-treated $CoFe_2O_4$ powder (b) and γ -Fe₂O₃ powder (c). Solid lines show the experimentally recorded curves, dashed lines show the theoretical fitting curves.

the Langevin dependence M(H). Heat treatment of the $CoFe_2O_4$ powder led to a considerable change of $\mu''(f)$. For this powder (Figure 5, b), the only one resonance curve at $f_0=8\,\mathrm{GHz}$ is observed. Actually, when using the fitting parameter $K\approx 6.5\cdot 10^4\,\mathrm{erg/cm^3}$ and mean powder size $d_3\approx 23\,\mathrm{nm}$, we get $\sigma=KV/k_BT=98\gg 1$ at room temperature. Figure 5, b shows the fitting curve based on expression (6). The experimental natural FMR curve of the γ -Fe₂O₃ powder has a relaxation type of absorption at $f_0=1.2\,\mathrm{GHz}$ (Figure 5, c). The fitting curve plotted using (5), is shown in Figure 5, c, and its fitting parameters listed in Table 2 agree quite well with the experimentally measured values (Table 1).

Thus, the main finding of the work is the experimental demonstration of heating of the cobalt ferrite nanopowder at 8.9 GHz due to the resonance absorption of the microwave energy in the intrinsic anisotropy field of particles. It should be emphasized that the possibility to achieve a high thermal effect by exciting the ferromagnetic resonance without using a bias field considerably simplifies a possible therapeutic application of magnetic resonance hyperthermia. With this technique, it is not necessary any longer to have electromagnets or permanent magnets and to control the conditions in which nanoparticles fall into resonance in the therapeutic treatment region.

4. Conclusion

The chemical deposition method was used to make the γ -Fe₂O₃ powders with $d_4 \approx 8$ nm, CoFe₂O₄, characterized by bimodal distribution $d_1 \approx 4 \, \text{nm}$ and $d_2 \approx 11 \, \text{nm}$. Heat treatment of the freshly prepared CoFe₂O₄ powder led to the increase in size to $d_3 \approx 23 \,\mathrm{nm}$. Magnetization curves were measured at room temperature to determine the magnetization of the prepared powders. Ferromagnetic resonance curves and dependences of powder heating temperatures on time were examined with microwave field energy absorption at 8.9 GHz with different magnetic field strengths. It was found that the maximum heating of the cobalt ferrite powders is achieved with the natural ferromagnetic resonance without an applied permanent magnetic field. Frequency dependences of the imaginary component of permeability $\mu''(f)$ were examined for the prepared powders without a permanent magnetic field to determine the natural ferromagnetic resonance frequency. $\mu''(f)$ of the freshly prepared CoFe₂O₄ powder were characterized by two features: a relaxation type absorption at $f_0=0.8\,\mathrm{GHz}$ and resonance absorption at $f_0=7.5\,\mathrm{GHz}$. The annealed CoFe₂O₄ powder had the resonance absorption at $f_0=8\,\mathrm{GHz}$. The γ -Fe₂O₃ powder had the relaxation type absorption at $f_0=1.2\,\mathrm{GHz}$. Using the theoretical expressions from [14] for magnetic susceptibility of a dispersion ferromagnetic material, magnetic parameters of the prepared powders were evaluated successfully. The observed effects may find a practical application in a new ferromagnetic-resonance particle heating method for magnetic hyperthermia.

Acknowledgments

The authors would like to thank the Krasnoyarsk Regional Center for Collective Use of the Federal Research Center-Krasnoyarsk Scientific Center, Siberian Branch of the Russian Academy of Sciences, for providing the measurement equipment.

Funding

The study was carried out within the framework of the research topic under the State Assignment of the Federal Research Center-Krasnoyarsk Scientific Center, Siberian Branch of the Russian Academy of Sciences.

Conflict of interest

The authors declare that they have no conflict of interest.

References

- E.C.S. Santos, J.A. Cunha, M.G. Martins, B.M. Galeano-Villar, R.J. Caraballo-Vivas, P.B. Leite, A.L. Rossi, F. Garcia, P.V. Finotelli, H.C. Ferraz. J. Alloys Compd. 879, 160448 (2021).
- [2] E.G. Fuller, H. Sun, R.D. Dhavalikar, M. Unni, G.M. Scheutz, B.S. Sumerlin, C. Rinaldi. ACS Appl. Polym. Mater. 1, 211 (2019).
- [3] M. Coïsson, G. Barrera, C. Appino, F. Celegato, L. Martino, A.P. Safronov, G.V. Kurlyandskaya, P. Tiberto. J. Magn. Magn. Mater. 473, 403 (2019).
- [4] Q.A. Pankhurst, N.T.K. Thanh, S.K. Jones, J. Dobson. J. Phys. D. Appl. Phys. 42, 224001 (2009).
- [5] J.-H. Lee, Y. Kim, S.-K. Kim. Sci. Rep. 12, 1 (2022)
- [6] J.H. Lee, B. Kim, Y. Kim, S.K. Kim. Sci. Rep. 11, 1 (2021).
- [7] A.G. Gurevich. Magnitnyi rezonans v ferritakh i antiferomagnetikakh. Nauka, M. (1973). 591 p. (in Russian).
- [8] S.V. Stolyar, O.A. Li, E.D. Nikolaeva, N.M. Boev, A.M. Vorotynov, D.A. Velikanov, R.S. Iskhakov, V.F. Piankov, Y.V. Knyazev, O.A. Bayukov, A.O. Shokhrina, M.S. Molokeev, A.D. Vasiliev. FTT 65, 6, 1006 (2023). (in Russian).
- [9] S. V. Stolyar, O.A. Li, A.M. Vorotynov, D.A. Velikanov, N.G. Maksimov, R.S. Iskhakov, V.P. Ladygina, A.O. Shokhrina. Bull. Russ. Acad. Sci. Phys. 88, 536 (2024).
- [10] T.V. Drokina. Metody fiziki v meditsine. Kransoyar. gos. un-t, Krasnoyarsk. (2005). 262 s. (in Russian).

- [11] I.A. Brezovich, W.J. Atkinson, M.B. Lilly. Cancer Res. 44, 4752 (1984).
- [12] D.G.Short, P.F.Terner. TIIER. 68, 157 (1980). (in Russian).
- [13] Y.L. Raĭkher, M.I. Shliomis. In book: Advances in Chemical Physics: Relaxation Phenomena in Condensed Matter, Volume 87 / Editor W. Coffey, published by John Wiley & Sons, Inc. (1994). P. 595.
- [14] Yu.L.Raikher, M.I.Shliomis. ZhETF. <u>6</u>7, *3*, 1060 (1974). (in Russian).
- [15] A.V. Izotov, B.A. Belyaev, N.M. Boev, A.V. Burmitskikh, G.V. Skomorokhov, S.M. Zharkov, P.N. Solovev. J. Alloys Compd. 900, 163416 (2022).
- [16] S.V.Salikhov, A.G.Savchenko, I.S.Grebennikov, I.S.Yurtov. Izvestiya RAN. Seriya fizicheskaya, 79, 1251 (2015). (in Russian).
- [17] A.P. Safronov, I.V. Beketov, S.V. Komogortsev, G.V. Kurlyandskaya, A.I. Medvedev, D.V. Leiman, A. Larrañaga, S.M. Bhagat. AIP Adv. 3, 052135 (2013).
- [18] S.V. Stolyar, O.A. Li, E.D. Nikolaeva, V.F. Piankov, A.M. Vorotynov, D.A. Velikanov, Y.V. Knyazev, O.A. Bayukov, R.S. Iskhakov, M.N. Volochaev. FMM 124, 2, 182 (2023). (In Russian).

Translated by E.Ilinskaya